Contents lists available at ScienceDirect

Behavioural Brain Research

Research report

Lateral frontal pole and relational processing: Activation patterns and connectivity profile

Bart Hartogsveld[a], Bob Bramson[a], Suhas Vijayakumar[a], A. Dilene van Campen[a], José P. Marques[a], Karin Roelofs[a], Ivan Toni[a], Harold Bekkering[a], Rogier B. Mars[a,b,*]

[a] Donders Institute for Brain, Cognition and Behaviour, Radboud University Nijmegen, 6525 EZ Nijmegen, The Netherlands
[b] Wellcome Centre for Integrative Neuroimaging, Centre for Functional MRI of the Brain (FMRIB), Nuffield Department of Clinical Neurosciences, John Radcliffe Hospital, University of Oxford, Oxford OX3 9DU, United Kingdom

ARTICLE INFO

ABSTRACT

The functional contribution of the lateral frontal cortex to behavior has been discussed with reference to several higher-order cognitive domains. In a separate line of research, recent studies have focused on the anatomical organization of this part of the brain. These different approaches are rarely combined. Here, we combine previous work using anatomical connectivity that identified a lateral subdivision of the human frontal pole and work that suggested a general role for rostrolateral prefrontal cortex in processing higher-order relations, irrespective of the type of information. We asked healthy human volunteers to judge the relationship between pairs of stimuli, a task previously suggested to engage the lateral frontal pole. Presenting both shape and face stimuli, we indeed observed overlapping activation of the lateral prefrontal cortex when subjects judged relations between pairs. Using resting state functional MRI, we confirmed that the activated region's whole-brain connectivity most strongly resembles that of the lateral frontal pole. Using diffusion MRI, we showed that the pattern of connections of this region with the main association fibers again is most similar to that of the lateral frontal pole, consistent with the observation that it is this anatomical region that is involved in relational processing.

1. Introduction

The human frontal cortex is often thought to be organized as a hierarchy, ranging from caudal motor areas, via caudal prefrontal areas involved in higher-order control processes, to the most rostral areas involved in the most abstract levels of control [1,2]. The anterior part of the prefrontal cortex sits at the top of this cortical hierarchy. It is often activated in tasks requiring the integration of outcomes of separate cognitive operations, especially when dealing with information outside direct environmental demands [3]. Anterior prefrontal cortex's functional interactions can reflect upcoming rather than current task demands [4]. However, although there has been substantial progress in the understanding of anterior prefrontal function, little is known about its anatomy. This is partly due to a lack of data from comparable regions in experimental animals. Recordings in the most anterior part of the cortex in the macaque monkey have been sparse and have yielded results that differ substantially from what was predicted based on human neuroimaging studies [5], leading some authors to suggest that part of the human anterior prefrontal cortex might be uniquely human [6].

To investigate the organization of the human frontal lobe, a number of recent studies used diffusion MRI to parcellate this part of the cortex based on structural connections to the rest of the brain. The logic of this approach is that cortical areas can be distinguished based on their unique pattern of connections, the so-called connectivity fingerprint [7]; [8]. Areas identified this way often are highly similar to those identified using traditional cytoarchitectonic methods [9]. A study by Neubert and colleagues revealed an area of the anterior prefrontal cortex located between the traditional area 10 and dorsolateral prefrontal cortex area 46, which was labeled lateral frontal pole (FPl) [10]. Although its connectivity fingerprint was similar to that of area 46, the two areas differed in their connectivity with medial frontal and inferior parietal cortex. Parallel work investigating the cytoarchitecture of the human frontal pole suggested a subdivision into a medial and a lateral part [11]. The lateral part was similar in location and had a similar connectivity profile to FPl. Importantly, Neubert and colleagues compared each human frontal area to areas in the macaque monkey. This revealed areas with similar connectivity profiles across species for the medial frontal pole and area 46, but no preferential match for the

human lateral frontal pole [10,27].

In a separate line of research, Bunge and colleagues reported an area of the left rostrolateral prefrontal cortex that is involved specifically in processing higher-order relations between mental representations [12]. This type of information processing goes beyond the learning of visuospatial, temporal, or semantic relationships that are first-order in nature, defining relations between relations. In a series of studies, they ruled out that activation of this part of prefrontal cortex was due to task difficulty and demonstrated its involvement across different paradigms [13,14]. Recently, Vendetti and Bunge [15] integrated these two research lines, suggesting that the lateral frontal pole identified by Neubert and colleagues is the same region that was activated during relational processing. Non-human primates can solve the kind of tasks used in humans to probe processing of higher-order relations, but might do so using alternative, often much less efficient strategies [16]. This suggests the presence of specializations for this type of information processing in the human lineage, possibly involving FPl. Consistent with this suggestion, integrating different domains of knowledge or abstracting away from familiar items to apply their rules to novel stimuli has been suggested to emerge only late in the human lineage [17].

Here we tested two suggestions originating from this idea. First, we aimed to test whether the region identified by Bunge and colleagues on functional grounds is indeed the same as the region Neubert and colleagues identified on anatomical grounds. We used the paradigm developed by Bunge and colleagues [12] identifying the lateral prefrontal locus for relational integration to localize this region in our participants (Fig. 1, left panel). Using resting state functional MRI we investigated the similarity in whole-brain functional connectivity of regions identified in the relational processing task with that of FPl and related regions, testing the hypothesis that the functional connectivity of FPl most closely matches that of the relational integration area (Fig. 1, right panel). Using diffusion MRI-based tractography we then determined the pattern of connections of the reported regions with the main association fibers of the brain and compared them with the patterns of different anterior prefrontal regions, again testing whether the pattern of FPl most closely matches the relational integration region (Fig. 1, right panel). Second, we reasoned that if this region's role in indeed characterized by the processing of higher-order relations we would expect this to be domain-general. Therefore, we also tested a variant of the relational integration paradigm using different stimuli, testing whether FPl is involved independent of the types of stimuli. Rather than using abstract shape stimuli, we presented face stimuli and asked participants to judge them on age and ethnicity. Together, this project thus tested the anatomical area involved in processing higher-order relations and its domain-generality.

2. Materials and methods

2.1. Participants and setup

19 healthy, right-handed males (age range 18–30 years) participated in the study after giving written informed consent according to the institutional guidelines of the local ethics committee (CMO region Arnhem-Nijmegen, the Netherlands). All participants had normal to corrected-to-normal vision. Data from three additional participants were discarded, as they did not perform above chance level in one of the task conditions.

During the experiment participants lay supine on the MRI scanner bed and observed visual stimuli projected through a mirror above the head coil. The presentation of the stimuli was controlled by a PC running Presentation software version 11.0 (http://www.neurobs.com). Motor responses were recorded through an MR-compatible button box, using the index and middle finger of the right hand.
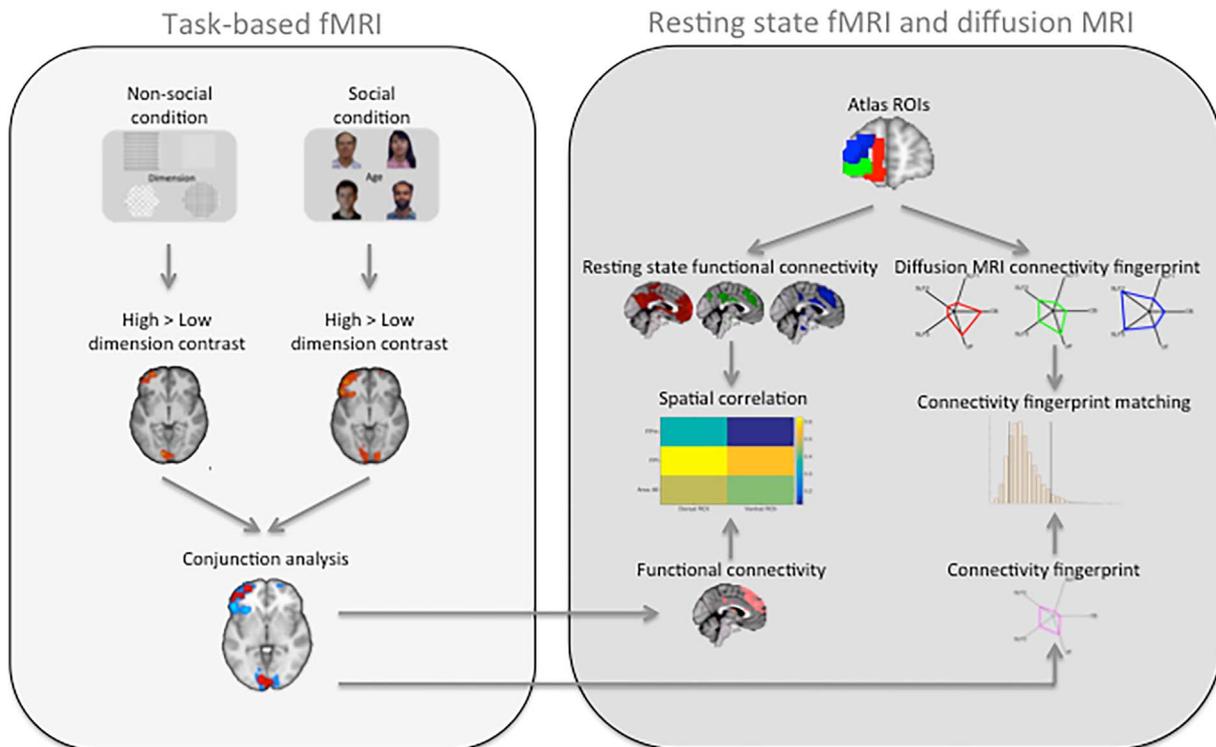
Fig. 1. Schematic overview of the different parts of the study and their relationship. The task-based functional part of the study (*left panel*) consisted of the relational integration task of Bunge and colleagues [9] (Non-social condition) and an extension using face stimuli (Social condition). In both cases we focused on the contrast of High versus Low dimension trials. We then calculated a conjunction of these two contrasts. The anatomical part of the study (*right panel*) consisted of whole-brain resting state functional connectivity and diffusion MRI tractography of atlas-based FPm, FPl, and area 46 regions of interest. The whole-brain resting state functional connectivity maps were compared to the same maps from the areas yielded by the conjunction analysis (*left column*). The diffusion MRI data was used to construct a connectivity fingerprint with five white matter tracts which was then matched to the same of the areas yielded by the conjunction analysis (*right column*).

2.2. Behavioral procedure

The task was a mixed blocked and event-related design, and consisted of two counterbalanced blocks, with 80 trials per block. In the different blocks, participants either performed a version of the task used by Bunge and colleagues [12] ('Non-social condition') or a similar task using face stimuli ('Social condition'). On each trial, participants had to make a judgement about the relation between stimuli ('Low dimension trials') or about the relation between stimulus relations ('High dimension trials'). Participants received both written and verbal task instructions and performed 10 practice trials before entering the scanner.

Participants were instructed that they would be presented with four images on the screen at the same time, divided into two pairs (upper pair with top left and top right image, lower pair with bottom left and bottom right image) (Fig. 2). Before these images were shown, a cue word would appear and stay on the screen. In the Non-social condition block, the cue words were "Shape" (20 trials) or "Texture" (20 trials) on the Low dimension trials, or "Dimension" (40 trials) on the High dimension trials. On the Low dimension trials participants had to determine whether there was a match on the dimension indicated by the the word in either the top or bottom pair, or both. On High dimension trials participants had to determine whether there was an equal match in both pairs (i.e., either a match on shape or match on texture in both pairs). The stimuli consisted of shapes (squares, circles, and hexagons) of different textures (dotted, striped, or grid) and different sizes (an irrelevant dimension).

In the Social condition block, the presented words were "Age" (20 trials) or "Ethnicity" (20 trials) on the Low dimension trials, or "Dimension" (40 trials) on the High dimension trials. The stimuli consisted of frontal profile faces belonging to three age categories (young < 30, middle 30–50, and old > 50 years of age), and three different ethnicity categories (Caucasian, Asian, and Middle-Eastern including Northern-African and Indian descent) belonging to both sexes (an irrelevant dimension). The face images were retrieved from the colour FERET database version 2, from the National Institute of Standards and Technology [18,19]. They were normalized in size, background, luminance, brightness, contrast and colour temperature using Adobe Photoshop CS6 (Adobe Systems, San Jose, CA). To ensure the images fit in the categories explained above, 16 participants assessed 247 images in a behavioral pilot experiment and only those stimuli with a correctness score exceeding 66 percent were used in the experiment.

In all trials participants were first presented with a fixation cross for 500 ms, after which the cue word appeared, joined after 1000 ms by the two stimulus pairs for a maximum of 5500 ms during which participants had time to respond. After the response a randomized inter-trial interval (1000–5000 ms, uniform distribution) was presented.

2.3. Image acquisition

Images were acquired on a 3 T Siemens Prisma MRI system, using a standard circular polarized head coil for radio-frequency transmission and signal reception (20 channel head/neck coil for T1 structural sequence, 32 channel head coil for the rest of the sequences). BOLD fMRI was acquired continuously during performance of each of the two task conditions. After both tasks a field map image was acquired. Diffusion MRI was recorded after completion of both task blocks. Resting state BOLD fMRI and structural T1 scans were acquired in a separate session on a different date, as was task data from an experiment not reported in this communication. Resting state BOLD fMRI acquisitions were followed by a field map.

2.3.1. Functional MRI

During both tasks, BOLD-sensitive functional images were acquired using a multiband sequence (acceleration factor 8 with GRAPPA method, TR 735 ms/TE 39 ms, interleaved acquisition, effective voxel size 2.4 × 2.4 × 2.4 mm, 64 slices, FoV 210 mm, orientation T > C − 16.0, phase encoding direction A ≫ P, flip angle 52°, distance factor 0%). Resting state images were acquired using the same sequence in a separate session, for 8.5 min. After each functional sequence field map images were acquired (flip angle 60°, TR 614 ms/TE 4.92 ms). All scans were aligned using an auto-align head scout sequence, comparing the images with the built-in brain atlas, to ensure coverage of the entire neocortex.

2.3.2. Diffusion MRI

Diffusion-weighted data were acquired using echo-planar imaging (GRAPPA acceleration factor 2, 65 2 mm-thick axial slices, voxel size of 2 × 2 x 2 mm, phase encoding direction A ≫ P, FoV 220 mm). 10 vols without diffusion weighting ($b = 0$ sxmm^{-2}), 30 isotropically distributed directions using a b-value of 750 sxmm^{-2}, and 60 isotropically distributed directions a b-value of 3000 sxmm^{-2} were acquired. A volume without diffusion weighting with reverse phase encoding (P ≫ A) was also acquired.

2.3.3. T1 structural

High-resolution anatomical images were acquired with a single-shot MPRAGE sequence (acceleration factor 2 with GRAPPA method, TR 2400 ms/TE 2.13 ms, effective voxel size 1 × 1 x 1 mm, 176 sagittal
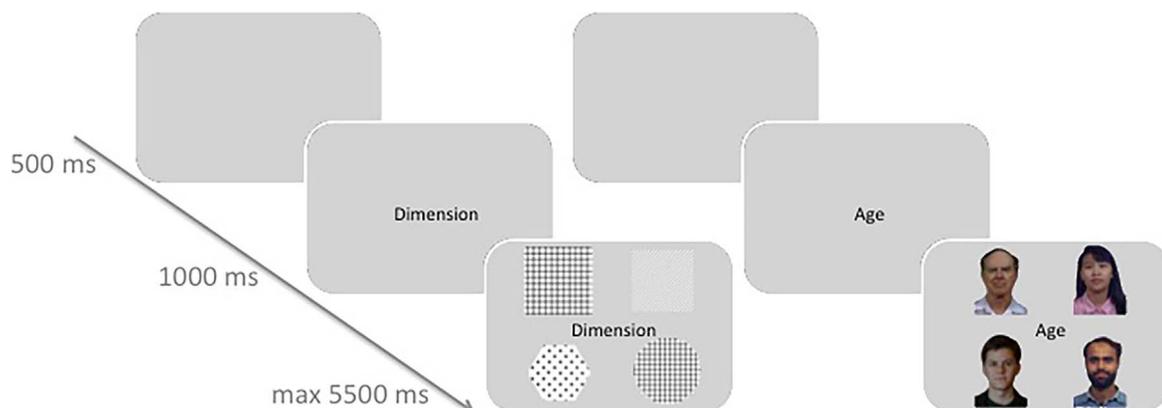
Fig. 2. Task protocol. Example trials of the Non-social Condition (High dimension trial, *left*) and the Social Condition (Low dimension, *right*). Each trial started with a 500 ms fixation. Then the cue word appeared, followed after 1000 ms by the two stimuli pairs. Subjects had a maximum of 5500 ms to respond. A 1000–5000 empty screen served as inter-trial interval.

slices, distance factor 50%, flip angle 8°, orientation A ≫ P, FoV 256 mm).

2.4. Image analysis

2.4.1. Task session

Functional MRI data processing was carried out using FEAT version 6.00, part of FSL (www.fmrib.ox.ac.uk/fsl). Data were motion corrected using MCFLIRT [20]. Fieldmap-based distortion correction of the functional images was carried out using FUGUE and registration to high-resolution structural and standard space images was carried out using linear registration. Registration from high resolution structural to standard space was then further refined using nonlinear registration. Additional preprocessing consisted of motion correction, removal of non-brain tissue, high-pass filtering using a 100 s cut-off, spatial smoothing using a Gaussian kernel of FWHM 5 mm, and grand-mean intensity normalization of the entire 4D dataset by a single multiplicative factor. Afterward, the functional data were manually denoised using probabilistic independent component analysis [21], identifying and regressing out obvious noise components [22], considering only the first 10 components of each participant that had the greatest impact to interfere with task data.

Time-series statistical analysis was carried out using FILM with local autocorrelation correction [23]. Statistical analysis was performed at two levels. At the first level, we used an event-related GLM approach for each participant. The data from the Non-social and Social runs were analyzed separately. The model consisted of three regressors: one capturing Low dimension trials to which the subject responded correctly, one capturing High dimension trials to which the subject responded correctly, and one capturing trials with erroneous responses. Events were time-locked to the presentation of the stimulus and modeled as having a duration from the appearance of the stimulus until the response. Regressors were convolved with a standard gamma function. The contrast of interest searched for regions more activated on High dimension as compared to Low dimension trials. On the second level, we used FSL's Local Analysis of Mixed Effects (FLAME 1) [24] with outlier deweighting [25] and tested the single group average. Z-statistic images were thresholded using clusters determined by Z > 2.3 and a corrected cluster significance threshold of $p = 0.05$ [26]. A conjunction of the group-level results was performed using the minimum statistic [27] and using clusters determined by Z > 2.3.

Activations were assigned to anatomical areas with the help of probabilistic atlases for visual cortex [28,29], inferior parietal cortex [9], superior parietal cortex [30], medial and ventral frontal cortex [31], and dorsal frontal cortex [32]. A region of interest was drawn using the Harvard-Oxford Structural atlas (https://fsl.fmrib.ox.ac.uk/fsl/fslwiki/Atlases).

2.4.2. Resting state fMRI data

Functional MRI data obtained during the resting state session were preprocessed in the same way as the task-based data, including motion correction, fieldmap correction, denoising, and registration. Subsequently, we used seed-based correlation analysis [33] to determine, in separate analyses, the resting state functional connectivity of each region reported in the task-based analyses. A $3 \times 3 \times 3$ voxel mask in MNI152 2 mm standard space was draw around the peak. The first eigen time series of the task region was extracted and correlated with the time course of each grey matter voxel while accounting for the time course of white matter and cerebrospinal fluid (cf. [34]. The resulting correlation maps were warped to MNI standard space, transformed using Fisher's r-to-z transform and subsequently tested at the group level using a voxel-wise GLM approach. The same was done for the lateral frontal pole (FPl), the neighboring medial frontal pole

(FPm), and area 46 as defined by the atlas of Neubert and colleagues [10] (thresholded at 25% of the population, mirrored to the left hemisphere and once Fig. 4, top left panel) to allow comparison to their functional connectivity networks.

2.4.3. Diffusion MRI data

We used diffusion MRI to assess whether the connectivity fingerprint of the areas reported in the task-based fMRI experiment was most similar to that of FPl or area 46 and FPm. Diffusion MRI data processing was carried out using FDT version 3.0, part of FSL (www.fmrib.ox.ac.uk/fsl). An additional $b = 0$ vol with reversed phase-encoding direction was used for TOPUP distortion correction [35]. Data were corrected for eddy currents and the results of TOPUP were used to correct the entire dataset. We used BedpostX to fit a crossing fiber model to the data [36] using a multi-shell extension to reduce overfitting of crossing fibers due to non-monoexponential diffusion decay [37]. Up to two fiber orientations per voxel were allowed. This produced voxel-wise posterior distributions of fiber orientations that were subsequently used in probabilistic tractography.

Seed regions were drawn in MNI152 2 mm standard space. To not bias the results we drew all masks within the same coronal section (y = −2) and used equally sized seeds placed in anatomical regions that should reliably contain the body of each tract. The seed region for the cingulum bundle (CB) was placed in the white matter underneath the cingulate sulcus (cf. [38], centered at [−8 −2 36]); those for the first, second, third branches of the superior longitudinal fascicle (SLF) were place in the superior, middle, and inferior frontal gyrus, respectively (cf. [39], centered at [−16 −2 54, −30 −2 38], and [−44 −2 26]); and that for the uncinate fascicle (UF) in the floor of the extreme capsule connecting the frontal and temporal lobes (cf. [40], centered at [−32 −2 −10]) (Fig. 5, middle left panel). The seed regions were warped to each subject's diffusion space and tractography was run from each of them using the default parameters of probtrackx2. Tracking was constrained by an exclusion mask between the two hemispheres and a coronal waypoint at y = 22 to only allow tracts to the ipsilateral frontal cortex. Tractograms were log transformed and normalized to the maximum value to allow for comparison between the different sized target areas and subjects (cf. [41]; [42]) and warped to standard space. We then created the connectivity fingerprints of FPl, FPm, and area 46 by counting how often any of the tractograms reached these areas as defined by the atlas of Neubert and colleagues [10] (thresholded at 25% of the population, mirrored to the left hemisphere and once dilated). The connectivity fingerprints of the areas resulting from the task-based fMRI experiment were constructed in a similar manner. Connectivity fingerprint matching was used to assess whether the task-based regions' fingerprints differed more from those of each of the atlas-based regions than expected. This technique uses a permutation testing framework to test whether the connectivity fingerprints differ by permuting the category label 10000 times [27].

3. Results

3.1. Behavioral data

A repeated measures ANOVA with levels CONDITION (Non-social vs Social) and DIMENSION (High dimension vs Low dimension) on the percentage correct responses showed that our manipulation was successful in that the High dimension trials were more difficult than the Low dimension trials (Non-social mean 93.0 (sem 2.2) vs 81.3 (3.8); Social 71.0 (2.0) vs 66.3 (1.7); main effect of DIMENSION $F(1,18) = 16.695, p = 0.001$). The Social condition was overall more difficult than the Non-social condition (main effect of CONDITION $F(1,18) = 63.332, p < 0.001$), but there was no interaction between the two

factors $F(1,18) = 3.732$, $p = 0.069$). A similar pattern was evident for the reaction times on correct trials (Non-social 1970 (119) vs 2386 (149) ms; Social 3123 (173) vs 3673 (204)) with main effects of DIMENSION ($F(1,18) = 43.416$, $p < 0.001$) and CONDITION ($F(1,18) = 103.646$, $p < 0.001$), but no interaction between the two factors ($F(1,18) = 1.938$, $p = 0.181$).

3.2. Functional imaging data

We set out to test the hypothesis that lateral frontal polar cortex shows more activation in the High dimension as compared to the Low dimension trials independent of stimulus type. In the Non-social condition this contrast resulted in four large clusters (Fig. 3, top left; Table 1). The first was a large cluster in the early visual cortex extending into Crus I of the cerebellum. Activation along the right intra-parietal sulcus had local maxima in inferior parietal areas PFt, PFm, and PGa and superior parietal area 7A. Two clusters were found in the frontal lobe. There was an extended cluster in the medial frontal cortex, with prominent local maxima in the rostral cingulate zone at the border with area 32d, in area 8m, and in pre-SMA, and a lateral cluster in the left hemisphere concentrated in the lateral frontal pole and extending into area 47m.

Activation for High as compared to Low dimension trials in the Social condition was much more extended (Fig. 3, top right; Table 1). The largest activation was located in the left lateral frontal cortex, with local maxima in the posterior medial frontal gyrus and the dorsal part of area 44, extending onto the pre-SMA medially, and frontally extending from area 9/46 V to FPl and 47 m. Activation in the right lateral pre-frontal cortex did not extend more ventrally than area 46. As in the Non-social condition, there was extended activation along the intra-parietal sulcus, albeit bilateral in this condition. Activation was also present in the cerebellum, including in Crus I that is connected to the frontal cortex [33]. It was noticeable that activation in the Social condition High dimension trials was much more extended than in the Non-social condition. This might in part be due to the fact that subjects experienced the Social condition as more difficult, as indicated by their longer reaction times and higher error rates.

The High vs Low dimensional contrast thus showed activation of the lateral prefrontal cortex in both the Non-social and Social condition. Overlapping the two activation maps shows a convergence in the left intra-parietal sulcus, the medial frontal cortex, and in the left lateral frontal cortex (Fig. 3, bottom left). A conjunction analysis focusing on a bilateral frontal pole region of interest as defined in the Harvard-Oxford structural atlas, which encompasses the medial and lateral frontal pole and parts of the dorsolateral prefrontal cortex, showed a cluster in the left lateral frontal pole (Fig. 3, bottom right). This cluster had two local maxima with $Z > 3$. The most dorsal at $[-30 \ 62 \ 12]$ is most likely to belong to area 46. The most ventral at $[-32 \ 58 \ -2]$ was assigned to FPl according to our previous parcellation-based atlases [10,31].

3.3. Resting state functional MRI data

In previous work, the lateral frontal pole was dissociated from the neighboring medial frontal pole and area 46 based on their connectivity
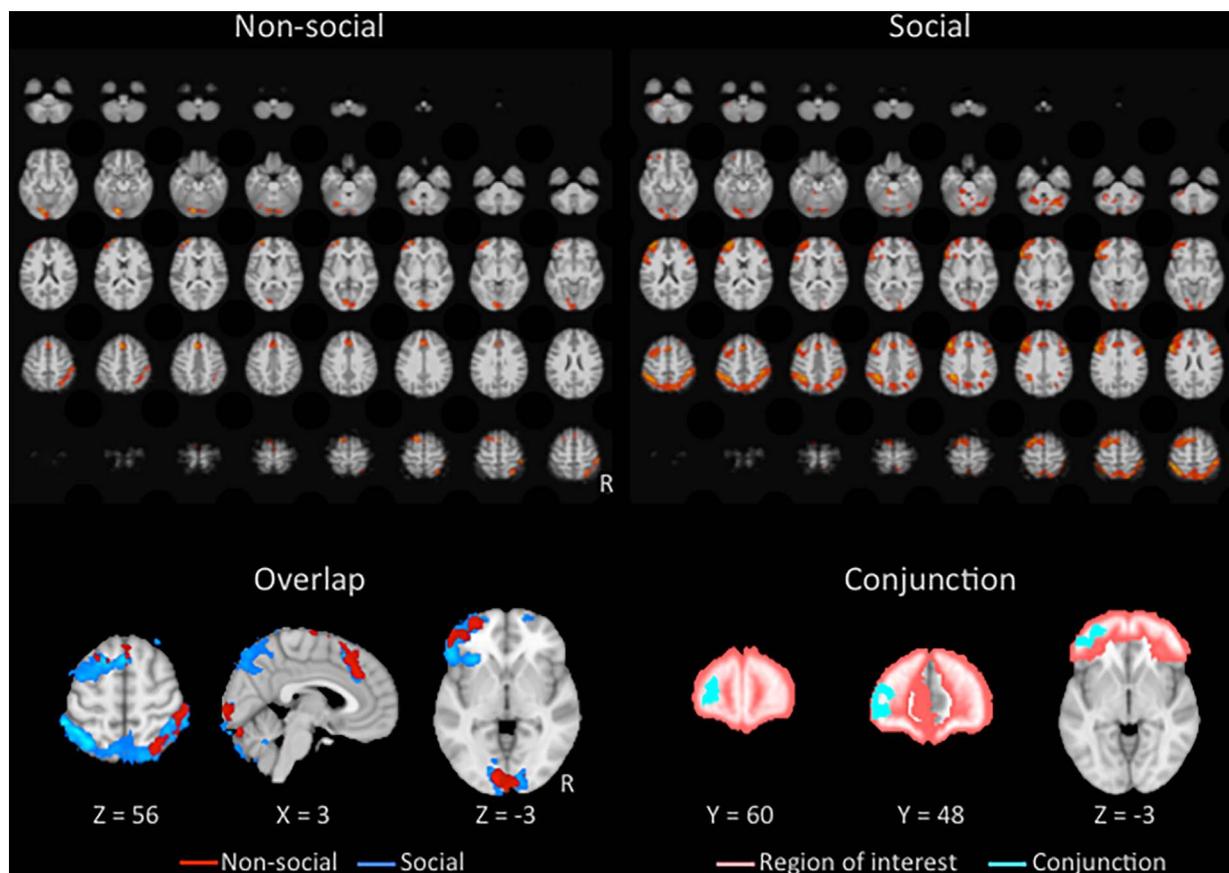
Fig. 3. Task-based fMRI results. Top row shows whole brain activations for the contrast of High dimension greater than Low dimension trials for the Non-social (*top left*) and Social (*top right*) trials (thresholded at Z > 2.3). The overlap of these two maps is displayed in the lower left. The lower right panel shows a conjunction analysis of these maps focusing on a region of interest of the frontal pole (*pink*), showing an extensive overlap in the lateral frontal pole, extending in to the dorsolateral frontal cortex (*cyan*).

Table 1
Functional activations for the High > Low Dimension contrast in both task conditions.

Anatomical region	MNI coordinates			Maximum Z-stat
	x	y	z	
Non-social High > Low Dimension				
Visual cortex and cerebellum cluster				
Visual cortex V3V	−12	−84	−18	3.77
Viusal cortex V2, BA18	−10	−90	−2	3.46
Visual cortex V1, BA17	−8	−86	2	3.41
Cerebellum Lobule VI	−26	−64	−30	3.16
Visual cortex V1, BA17	8	−94	0	3.12
Cerebellum Crus I	12	−84	−24	2.94
Medial frontal cluster				
Area 8m	−6	26	48	3.98
Pre-SMA	−16	18	66	3.78
Premotor cortex, BA6	0	16	60	3.78
Cingulate cortex, RCZa	0	32	34	3.59
Cingulate cortex, area 32d	−4	32	32	3.59
Area 8m	4	30	40	3.35
Parietal cluster				
Inferior parietal lobule PFt	54	−34	60	3.62
Superior parietal lobule 7A	34	−60	64	3.37
Superior parietal lobule 7A	34	−64	58	3.26
Inferior parietal lobule PFm	52	−42	56	2.68
Superior parietal lobule 7PC	42	−52	66	2.60
Inferior parietal lobule PGa	46	−50	50	2.58
Lateral prefrontal cluster				
Lateral frontal pole (FPl)	−28	64	12	3.51
Lateral frontal pole (FPl)	−28	60	6	3.51
Lateral frontal pole (FPl), Area 46	−32	58	−2	3.25
Lateral frontal pole (FPl)	−52	50	−4	3.15
Area 47m	−40	44	−6	2.99
Area 47m	−52	48	12	2.96
Social High > Low Dimension				
Frontal cluster				
Area 9/46V	−44	26	36	4.39
Pre-SMA	−2	20	48	4.36
Area 44d	−54	18	28	4.26
Anterior dorsal premotor cortex	−26	12	64	4.24
Area 9/46V	−44	32	42	4.23
Area 9/46V	−46	34	38	4.18
Parietal cluster				
Inferior parietal lobule PFm	−56	−42	56	4.80
Inferior parietal lobule PFt/PFm	−44	−52	56	4.76
Superior parietal lobule 7A	−34	−60	56	4.64
Inferior parietal lobule PGa	−40	−64	58	4.64
Inferior parietal lobule PGa	−38	−46	36	4.31
Superior parietal lobule 7A	42	−56	64	4.30
Visual cortex and cerebellum cluster				
Cerebellum Crus I	34	−64	−32	3.75
Brain stem	−8	−38	−24	3.65
Visual cortex V1, BA17	14	−90	−4	3.64
Cerebellum lobule X	−24	−36	−42	3.59
Cerebellum lobule VI	24	−64	−32	3.57
Visual cortex V1, BA17	12	−88	0	3.51
Lateral prefrontal cluster				
Area 44d	56	16	32	4.18
Area 9/46V	40	30	40	3.35
Area 9/46V	42	36	44	3.16
Area 46	34	64	20	3.11
Area 9/46V	42	40	42	3.11
Area 9/46D	34	36	54	3.04

with the rest of the brain. We calculated the whole-brain functional connectivity of each region (Fig. 4 top right). Compared to FPm, the connectivity of which resembled that of the default mode network in its strong medial posterior and medial prefrontal loci, FPl connectivity was more restricted to the posterior mid-cingulate and dorsomedial prefrontal cortex. FPl also showed more extended connectivity with bilateral posterior IPL. Compared to FPl, area 46 functional connectivity was found in the middle part of the cingulate and was more extensive in dorsomedial prefrontal cortex. Connectivity in the IPL extended more anteriorly for area 46 than for FPl.

Functional connectivity of the two regions of interest (ROIs) found in the task-based experiments are displayed in Fig. 4 (bottom right). Both showed connectivity with the dorsomedial prefrontal cortex, posterior part of the cingulate, and posterior part of the IPL. To investigate the similarity of the connectivity maps of the two ROIs with those of the three atlas-based region, we calculated the spatial correlation for each subject and averaged across the group. This showed that for both ROIs, the functional connectivity pattern was most similar to that of the FPl (Fig. 4, bottom left).
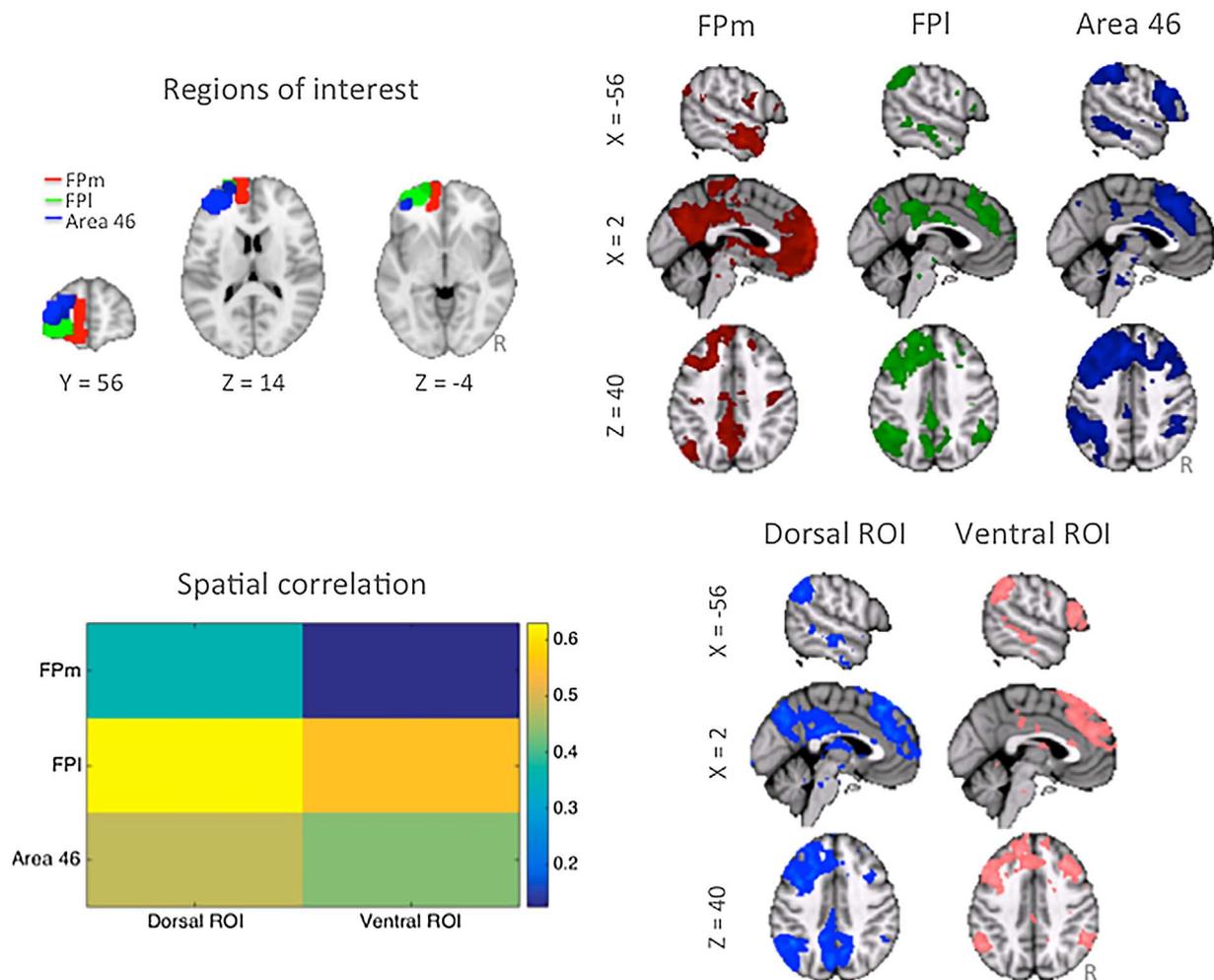
Fig. 4. Resting state functional connectivity results. *Top left* displays seed regions of atlas-based areas FPm, FPl, and area 46 and *top right* displays their whole-brain functional connectivity (thresholded at Z > 3 for display purposes). *Bottom right* displays whole-brain functional connectivity of the two local maxima of the conjunction analysis (thresholded at Z > 3 for display purposes). *Bottom left* depicts the spatial correction between the connectivity maps of the atlas-based regions and the task-based regions of interest shows that both loci have a pattern most similar to that of FPl.

3.4. Diffusion MRI data

To corroborate the resting state fMRI results, we used diffusion MRI tractography to construct connectivity fingerprints of these areas. We performed tractography seeded in the bodies of cingulum bundle (CB), the three branches of the superior longitudinal fascicle (SLF1, SLF2, SLF3), and the uncinate fascicle (UF) in the left hemisphere. We then assessed how often the tractograms of these tracts passed through target regions in FPm, FPl, and area 46. Area 46 was distinguished by having the strongest connectivity with the superior longitudinal fascicle, while FPm had the strongest connectivity with the cingulum bundle (Fig. 5, middle).

Similar connectivity fingerprints were constructed for the dorsal and ventral areas from the conjunction analysis described in the previous section. These fingerprints were compared to those of FPm, FPl, and area 46. The dorsal area's connectivity fingerprint (Fig. 5, middle, in cyan) differed significantly from that of FPm ($p = 0.005$; Fig. 5, top left), but not from either FPl ($p = 0.348$; Fig. 5, top middle) or area 46 ($p = 0.119$; Fig. 5, top right). In contrast, the connectivity fingerprint of the ventral area (Fig. 5, middle, in magenta) differed from both FPm ($p = 0.0174$; Fig. 5, bottom left) and–marginally–area 46 ($p = 0.047$; Fig. 5, bottom right), but not from FPl ($p = 0.842$; Fig. 5, bottom middle).

4. Discussion

We set out to test whether the lateral frontal pole (FPl) is activated in higher-order relational processing independent of stimulus domain and whether this part of the brain is the same as that identified in previous anatomical studies of prefrontal cortex. We replicated the results of Bunge et al. [12], showing that left FPl was active during processing of higher-order relations between visuospatial stimuli judged on shape and texture. An overlapping part of frontal cortex was active during processing of relations between faces judged on age and ethnicity. The conjunction analysis showed an extended region of activation, with a dorsal local maximum located in territory we assigned to area 46 and a ventral maximum we assigned to FPl based on previously published atlases. In the same subjects, we established the whole-brain resting state functional connectivity profiles of the subparts of lateral prefrontal cortex activated in the task and compared them with the profiles of atlas-based FPl and neighboring medial frontal pole and area 46. The task-activated regions had a connectivity profile most similar to that of FPl. We then used diffusion MRI tractography to investigate which association fibers reached the task-based regions, creating their structural connectivity fingerprint. These were compared to the fingerprints of FPl, FPm, and area 46. This showed that the ventral ROI differed significantly from FPm and area 46, but not FPl. The dorsal ROI connectivity fingerprint differed from FPm, but not from both FPl and area 46. In summary, we conclude that activation of
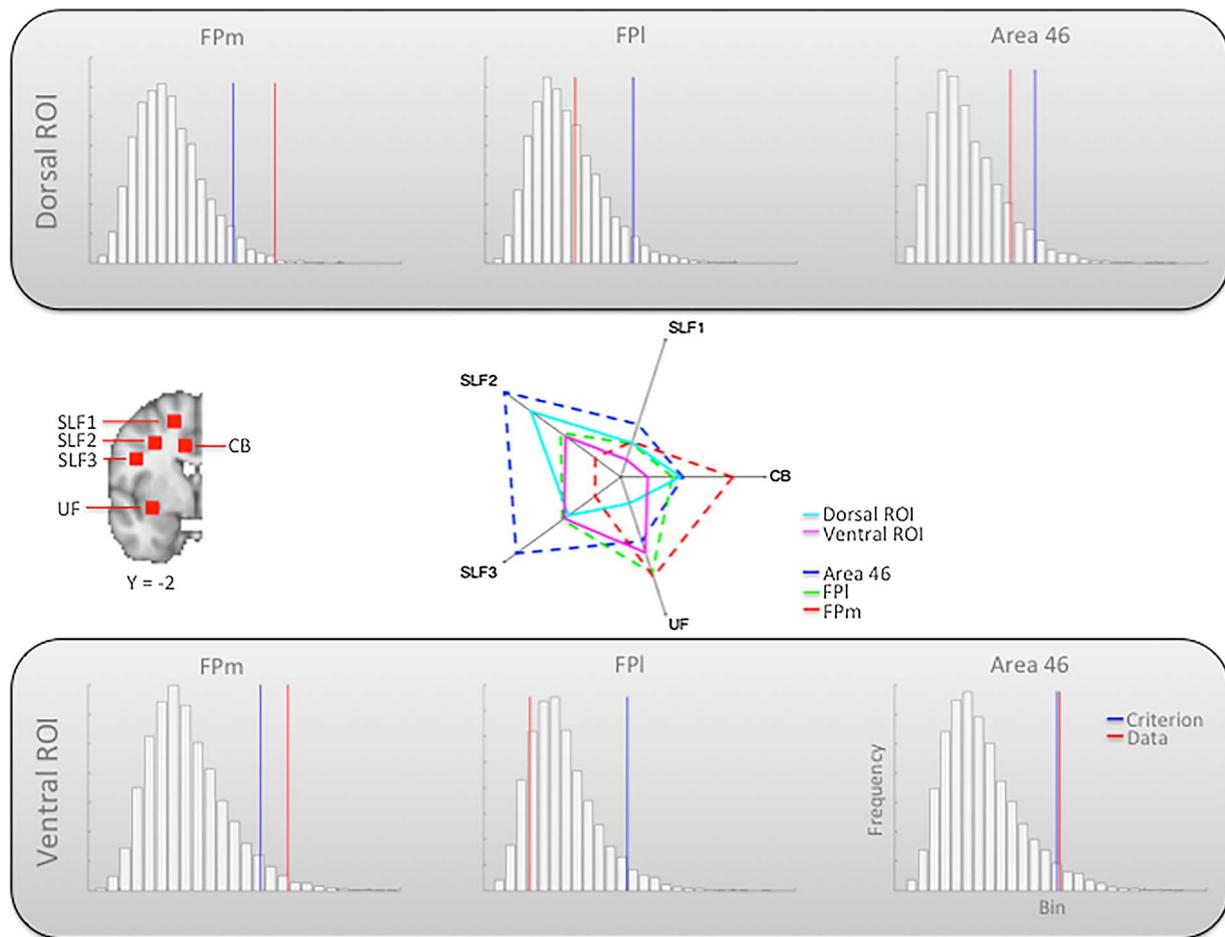
Fig. 5. Tractography results. *Middle panel* shows the connectivity fingerprints of atlas-based FPm, FPl, and area 46 and the two task based regions of interest (ROIs) with five association tracts (CB: cingulum bundle; SLF: superior longitudinal fascicle; UF: uncinate fascicle). Axes indicate connectivity strengths averaged across the group. Left-most middle panel shows the location of the white matter regions of interest. Top and bottom row histograms show the results of the permutation tests, assessing whether the observed data (red lines) is more or less different from the atlas-based area than criterion (blue line). (For interpretation of the references to colour in this figure legend, the reader is referred to the web version of this article.)

lateral prefrontal cortex during processing of higher-order relations occurs in an extended territory of the left hemisphere that includes FPl, independent on the type of visual stimuli used.

The task used in the present study was explicitly chosen to replicate the existing literature on prefrontal cortex activation in relational integration paradigms. Although this approach was successful, it does mean that there are certain inferences we cannot draw from the present data. For instance, as expected the High dimension condition was more difficult than the Low dimension condition. The current data cannot rule out that the frontal cortex activation is driven by this effect of difficulty. However, we chose this paradigm specifically because since Bunge and colleagues have validated the role of the lateral frontal pole it in a number of additional experiments, showing that the its role generalizes across experimental paradigms and is not driven by confounding factors (reviewed in [15]). One study in particular showed that while activation in a working memory task scaled with difficulty in dorsolateral prefrontal cortex, this was not the case for rostrolateral prefrontal cortex [13].

The present results indicate a domain-general role for FPl. Activation of the same parts of lateral prefrontal cortex was present during the High dimension trials in both the Non-social and Social blocks, suggesting that this part of the brain is involved in processing higher-order relationships independent of the type of visual information or the content of the relationship. This extends earlier findings by Wendelken et al. [43] showing involvement of rostrolateral prefrontal cortex in visuospatial and semantic versions of the relational integration task. FPl activation was also shown in a meta-analysis of relational

processing task activations [15]. An interesting question is whether this is the same area that shows increases in activation in tasks not explicitly designed to probe relational processing. Our earlier parcellation studies suggested that anatomically defined FPl overlaps with activation coding value of unchosen options in decision-making tasks [44]. This decision-making activity, in turn, has been interpreted in terms of comparing representations in a similar fashion as in the relational integration task [45]. Future studies might apply our current approach of combing task-based activation and anatomical data with paradigms shown to activate lateral prefrontal cortex in a wider range of circumstances, such as overcoming emotional biases [46].

We have used function connectivity of the task-based regions with the rest of the brain to establish whether whole-brain connectivity is similar to that of the lateral frontal pole, as determined previously. We emphasize that this approach aims to use function connectivity as a stable measure of a region's place in the larger cerebral network, rather than time-varying interactions during task performance as in the case of effective connectivity [47]. Although the networks found using resting state functional connectivity can show similarities to the sets of regions that interact during task performance [48], the focus here is on defining a region's place in the architecture of the brain. Both resting state fMRI and diffusion MRI rely on indirect observations that are only partially indicative of anatomical connections as identified using gold standard tracer methods. The two methods, however, suffer from different and in some cases opposite problems, and both have been demonstrated to be highly replicable. The current approach is therefore able to make reliable inferences on some aspects of the anatomy of cortical regions, even

without direct reference to tracer data, which is impossible to obtain in the living, human brain (see Smith et al. [49] for a similar approach).

Here, we have concentrated on group-level activation and connectivity patterns. It has recently been demonstrated that both diffusion MRI tractography [50] and resting state functional connectivity [51,52] can predict the loci of task activations in individuals. This is particularly interesting in the light of findings that anterior prefrontal activation during relational processing emerges late during development and correlates with structural changes in connected parts of parietal cortex [53]. Beyond connectivity, a better appreciation of the anatomy of individual brains can lead to better localization of task-based activations [54,55]. An extension of the current work will be to establish the relationship between structure and function at the level of the individual.

Relating task-based loci to specific anatomical regions is of course more than simple book keeping. The connectivity fingerprint is not only a unique identifier of a cortical region, it also provides clues concerning the information a region receives and the influence it can exert. In their original paper on connectivity fingerprints, Passingham and colleagues [7] illustrated the relationship between areas' connections and their neurons' response properties. Using this line of argument, in the study of motivational and cognitive control the connections of different prefrontal regions have been a vital ingredient in various proposals on the relationship between medial and lateral prefrontal cortex and the hierarchical organization of regions along prefrontal's rostro-caudal axis [56,2,57]. Moreover, recent debates about the function of the anterior cingulate cortex (ACC) in cognitive control have relied on anatomical arguments to demonstrate that human ACC is similar to that of the macaque and has access to information useful to a region involved in foraging decisions [58]. In summary, understanding connectional anatomy is a vital tool in understanding the neural basis of motivational and cognitive control.

As discussed in the Introduction, non-human primates have difficulty with the fast processing of relations between cognitive representations that humans are capable of. The finding that the lateral frontal pole might not have a clear homolog in the macaque monkey brain and the current confirmation that this area overlaps with the region that is activated during relational processing suggest it might be involved in this human ability. This is not to suggest that this area suddenly appeared *de novo* in the human brain, as it is known that evolution of cortical specializations is much more complicated [59]. Recent work on the evolution of prefrontal cortex has emphasized the role of its different parts in performing particular computations that aided its owner in dealing with the specific challenges presented by his ecological niche [60,61]. We hope that the present work, linking a particular anatomical region in the human brain to a specific function, can c inform this approach.

Conflict of interest

The authors declare no competing financial interests.

Acknowledgements

References

[1] M. Petrides, Lateral prefrontal cortex: architectonic and functional organization, Philos. Trans. R Soc. Lond. B Biol. Sci. 360 (2005) 781–795.

[2] D. Badre, M. D'Esposito, Is the rostro-caudal axis of the frontal lobe hierarchical? Nat. Neurosci. 10 (2009) 659–669.

[3] E. Koechlin, A. Hyafil, Anterior prefrontal cortex and the limits of human decision-making, Science 318 (2007) 594–598.

[4] K. Sakai, R.E. Passingham, Prefrontal interactions reflect future task operations,

[5] S. Tsujimoto, A. Genovesio, S.P. Wise, Frontal pole cortex: encoding ends at the end of the endbrain, Trends Cogn. Sci. 15 (2011) 169–176.

[6] E. Koechlin, Frontal pole function: what is specifically human? Trends Cogn. Sci. 15 (2011) 241.

[7] R.E. Passingham, K.E. Stephan, R. Kotter, The anatomical basis of functional localization in the cortex, Nat. Rev. Neurosci. 3 (2002) 606–616.

[8] H. Johansen-Berg, T.E. Behrens, M.D. Robson, I. Drobnjak, M.F. Rushworth, J.M. Brady, S.M. Smith, D.J. Higham, P.M. Matthews, Changes in connectivity profiles define functionally distinct regions in human medial frontal cortex, Proc. Natl. Acad. Sci. U. S. A. 101 (2004) 13335–13340.

[9] R.B. Mars, S. Jbabdi, J. Sallet, J.X. O'Reilly, P.L. Croxson, E. Olivier, M.P. Noonan, C. Bergmann, A.S. Mitchell, M.G. Baxter, T.E. Behrens, H. Johansen-Berg, V. Tomassini, K.L. Miller, M.F. Rushworth, Diffusion-weighted imaging tractography-based parcellation of the human parietal cortex and comparison with human and macaque resting-state functional connectivity, J. Neurosci. 31 (2011) 4087–4100.

[10] F.X. Neubert, R.B. Mars, A.G. Thomas, J. Sallet, M.F. Rushworth, Comparison of human ventral frontal cortex areas for cognitive control and language with areas in monkey frontal cortex, Neuron 81 (2014) 700–713.

[11] S. Bludau, S.B. Eickhoff, H. Mohlberg, S. Caspers, A.R. Laird, P.T. Fox, A. Schleicher, K. Zilles, K. Amunts, Cytoarchitecture, probability maps and functions of the human frontal pole, Neuroimage 93 (2014) 260–275.

[12] S.A. Bunge, E.H. Helskog, C. Wendelken, Left, but not right, rostrolatral prefrontal cortex meets a stringent test of the relational integration hypothesis, Neuroimage 46 (2009) 338–342.

[13] C. Wendelken, S.A. Bunge, C.S. Carter, Maintaining structural information: an investigation into functions of parietal and lateral prefrontal cortices, Neuropsychologica 46 (2008) 665–678.

[14] C. Wendelken, S.A. Bunge, Transitive inference: distinct contributions of rostrolateral prefrontal corte and the hippocampus, J. Cogn. Neurosci. 22 (2009) 837–847.

[15] M.S. Vendetti, S.A. Bunge, Evolutionary and developmental changes in the lateral frontoparietal network: a little goes a long way for higher-level cognition, Neuron 84 (2014) 906–917.

[16] D.C. Penn, K.J. Holyoak, D.J. Povinelli, Darwin's mistake: explaining the discontinuity between human and nonhuman minds, Behav. Brain Sci. 3 (2008) 109–178.

[17] S. Mithen, The Prehistory of Mind. A Search for the Origins of Art, Religion and Science, Orion Books, London, 1998.

[18] P.J. Phillips, H. Wechsler, J. Huang, P. Rauss, The FERET database and evaluation procedure for face recognition algorithms, Imaging Vision Comput. J. 16 (1998) 295–306.

[19] P.J. Phillips, H. moon, S.A. Rizvi, P.J. Rauss, The FERET evaluation methodology for face recognition algorithms, IEEE Trans. Pattern Anal. Mach. Intell. 22 (2000) 1090–1104.

[20] M. Jenkinson, P.R. Bannister, J.M. Brady, S.M. Smith, Improved optimisation for the robust and accurate linear registration and motor correction of brain images, Neuroimage 17 (2002) 825–841.

[21] C.F. Beckmann, S.M. Smith, Probabilistic independent component analysis for functional magnetic resonance imaging, IEEE Trans. Med. Imaging 23 (2004) 137–152.

[22] R.E. Kelly, G.S. Alexopoulos, Z. Wang, F.M. Gunning, C.F. Murphy, S.S. Morimoto, D. Kanellopoulos, Z. Jia, K.O. Lim, M.J. Hoptman, Visual inspection of independent components: defining a procedure for artifact removal from fMRI data, J. Neurosci. Methods 198 (2010) 233–245.

[23] M.W. Woolrich, B.D. Ripley, J.M. Brady, S.M. Smith, Temporal autocorrelation in univariate linear modelling of fMRI data, Neuroimage 1 (2001) 1370–1386.

[24] M.W. Woolrich, T.E.J. Behrens, C.F. Beckmann, M. Jenkinson, S.M. Smith, Multilevel linear modelling for fMRI group analysis using Bayesian inference, Neuroimage 21 (2004) 1732–1747.

[25] M.W. Woolrich, Robust group analysis using outlier inference, Neuroimage 41 (2008) 286–301.

[26] K.J. Worsley, Statistical analysis of activation images, in: P. Jezzard, P.M. Matthews, S.M. Smith (Eds.), Functional MRI: An Introduction to Methods, Oxford University Press, Oxford, 2001.

[27] T. Nichols, M. Brett, J. Andersson, T. Wager, J.B. Poline, Valid conjunction inference with the minimum statistic, Neuroimage 25 (2005) 653–660.

[28] K. Amunts, A. Malikovic, H. Mohlberg, T. Schormann, K. Zilles, Brodmann's areas 17 and 18 brought into stereotaxic space– where and how variable? Neuroimage 11 (2000) 66–84.

[29] C. Rottschy, S.B. Eickhoff, A. Schleicher, H. Mohlberg, M. Kujovic, K. Zilles, K. Amunts, Ventral visual cortex in humans: cytoarchitectonic mapping of two extrastriate areas, Hum. Brain Mapp. 28 (2007) 1045–1059.

[30] F. Scheperjans, S.B. Eickhoff, L. Hömke, H. Mohlberg, K. Hermann, K. Amunts, K. Zilles, Probabilistic maps, morphometry, and variability of cytoarchitectonic areas in the human superior parietal cortex, Cereb. Cortex 18 (2008) 2141–2157.

[31] F.X. Neubert, R.B. Mars, J. Sallet, M.F.S. Rushworth, Connectivity reveals relationship of brain areas for reward-guided learning and decision making in human and monkey frontal cortex, Proc. Natl. Acad. Sci. U. S. A. 112 (2015) E2695–E2704.

[32] J. Sallet, R.B. Mars, M.P. Noonan, F.X. Neubert, S. Jbabdi, J.X. O'Reilly, N. Filippini, A.G. Thomas, M.F. Rushworth, The organization of dorsal frontal cortex in humans and macaques, J. Neurosci. 33 (2013) 12255–12274.

[33] J.X. O'Reilly, C.F. Beckmann, V. Tomassini, N. Ramnani, H. Johansen-Berg, Distinct and overlapping functional zones in the cerebellum defined by resting state functional connectivity, Cereb. Cortex 20 (2010) 953–965.

[34] R.B. Mars, J. Sallet, U. Schüffelgen, S. Jbabdi, I. Toni, M.F. Rushworth, Connectivity-based subdivisions of the human right temporoparietal junction area: evidence for different areas participating in different cortical networks, Cereb. Cortex 22 (2012) 1894–1903.

[35] J.L.R. Andersson, S. Skare, J. Ashburner, How to correct susceptibility distortions in spin-echo echo-planar images: application to diffusion tensor imaging, Neuroimage 20 (2003) 870–888.

[36] T.E. Behrens, H. Johansen-Berg, S. Jbabdi, M.F. Rushworth, M.W. Woolrich, Probabilistic diffusion tractography with multiple fibre orientations: what can we gain? Neuroimage 34 (2007) 144–155.

[37] S. Jbabdi, S.N. Sotiropoulos, A.M. Savio, M. Grana, T.E.J. Behrens, Model-based analysis of multishell diffusion MR data for tractography: how to get over fitting problems, Magn Res. Med. 68 (2012) 1846–1855.

[38] J.D. Schmahmann, D.N. Pandya, Fiber Pathways of the Brain, Oxford University Press, Oxford, 2009.

[39] M. Thiebaut de Schotten, S. Kinkingnehun, C. Delmaire, S. Lehericy, H. Duffau, L. Thivard, E. Volle, R. Levy, B. Dubois, P. Bartolomeo, Visualization of dis-connection syndromes in humans, Cortex 44 (2008) 1097–1103.

[40] M. Thiebaut de Schotten, F. Dell'Acqua, R. Valabregue, M. Catani, Monkey to human comparative anatomy of the frontal lobe association tracts, Cortex 48 (2012) 82–96.

[41] R.B. Mars, S. Foxley, S. Jbabdi, J. Sallet, M.P. Noonan, F.X. Neubert, J.L. Andersson, L. Verhagen, P.L. Croxson, R.I.M. Dunbar, A. Khrapichev, N. Sibson, K.L. Miller, M.F.S. Rushworth, The extreme capsule fiber complex in humans and macaques: a comparative diffusion MRI tractography study, Brain Struct. Funct. 221 (2016) 4059–4071.

[42] R.B. Mars, L. Verhagen, T.E. Gladwin, F.X. Neubert, J. Sallet, M.F.S. Rushworth, Comparing brains by matching connectivity profiles, Neurosci. Biobehav. Rev. 60 (2016) 90–97.

[43] C. Wendelken, D. Chung, S.A. Bunge, Rostrolateral prefrontal cortex: domain-gen-eral or domain-sensitive? Hum. Brain Mapp. 33 (2012) 1952–1963.

[44] E.D. Boorman, T.E. Behrens, M.W. Woolrich, M.F. Rushworth, How green is the grass on the other side? frontopolar cortex and the evidence in favor of alternative courses of action, Neuron 62 (2009) 733–743.

[45] S.A. Bunge, C. Wendelken, Comparing the bird in the hand with the ones in the bush, Neuron 62 (2009) 609–611.

[46] I. Volman, I. Toni, L. Verhagen, K. Roelofs, Endogenous testosterone modulates prefrontal-amygdala connectivity during social emotional behavior, Cereb. Cortex 21 (2011) 2282–2290.

[47] K.J. Friston, Functional and effective connectivity: a review, Brain Connect. 1 (2011) 13–36.

[48] S.M. Smith, P.T. Fox, K.L. Miller, D.C. Glahn, P.M. Fox, C.E. Mackay, N. Filippini, K.E. Watkins, R. Toro, A.R. Laird, C.F. Beckmann, Correspondence of the brain's functional architecture during activation and rest, Proc. Natl. Acad. Sci. U. S. A. 106 (2009) 13040–13045.

[49] A.T. Smith, A.L. Beer, M. Furlan, R.B. Mars, Connectivity of the cingulate sulcus visual area (CSv) in the human cerebral cortex, Cereb. Cortex (2017) (in press).

[50] D.E. Osher, R.R. Saxe, R. Koldewyn, J.D. Gabrieli, N. Kanwisher, Z.M. Saygin, Structural connectivity fingerprints predict cortical selectivity for multiple visual categories across cortex, Cereb. Cortex 26 (2016) 1668–1683.

[51] D. Bzdok, G. Varoquaux, O. Grisel, M. Eickenberg, C. Poupon, B. Thirion, Formal models of the network co-occurrence underlying mental operations, PLoS Comput. Biol. 12 (2016) e1004994.

[52] I. Tavor, O. Parker Jones, R.B. Mars, S.M. Smith, T.E. Behrens, S. Jbabdi, Task-free MRI predicts individual differences in brain activity during task performance, Science 352 (2016) 216–220.

[53] C. Wendelken, E.D. O'Hare, K.J. Whitaker, E. Ferrer, S.A. Bunge, Increased func-tional selectivity over development in rostrolateral prefrontal cortex, J. Neurosci. 31 (2011) 17260–17268.

[54] C. Amiez, R. Neveu, D. Warrot, M. Petrides, K. Knoblauch, E. Procyk, The location of feedback-related activity in the midcingulate cortex is predicted by local mor-phology, J. Neurosci. 33 (2013) 2217–2228.

[55] Y. Li, G. Sescousse, C. Amiez, J.C. Dreher, Local morphology predicts functional organization of experienced value signals in the human orbitofrontal cortex, J. Neurosci. 35 (2015) 1648–1658.

[56] M. Petrides, D.N. Pandya, Association pathways of the prefrontal cortex and func-tional observations, in: D.T. Stuss, R.T. Knight (Eds.), Principles of Frontal Lobe Function, Oxford University Press, New York, 2002, pp. 31–50.

[57] F. Kouneiher, S. Charron, E. Koechlin, Motivational and cognitive control in the human prefrontal cortex, Nat. Neurosci. 12 (2009) 939–945.

[58] N. Kolling, M.K. Wittmann, T.E.J. Behrens, E.D. Boorman, R.B. Mars, M.F.S. Rushworth, Value, search, persistence and model updating in anterior cin-gulate cortex, Nat. Neurosci. 10 (2016) 1280–1285.

[59] L. Krubitzer, J. Kaas, The evolution of the neocortex in mammals: how is phenotypic diversity generated? Curr. Opin. Neurobiol. 15 (2005) 444–453.

[60] R.E. Passingham, S.P. Wise, The Neurobiology of the Prefrontal Cortex: Anatomy, Evolution, and the Origin of Insight, Oxford Univeristy Press, Oxford, 2012.

[61] E. Koechlin, An evolutionary computational theory of prefrontal executive function in decision-making, Philos. Trans. R. Soc. Lond. B 369 (2014) 1655.